Effect of structure and texture on infiltration flow pattern during flood irrigation

Jae Gon Kim · Chul-Min Chon · Jin-Soo Lee

Abstract Understanding the flow pattern of water and solute in subsurface soils is critically important in the fields of agricultural and environmental sciences. Dye tracer tests using a flood irrigation of Brilliant Blue FCF solution (5 g l^{-1}) and excavation method was performed to investigate the effect of texture and structure on the infiltration pattern at three different field soils developed from granite (GR), gneiss (GN) and limestone (LS). The GR soil showed a homogeneous matrix flow in the surface soil with weak, medium granular structure and a macropore flow along pegmatitic vein and plant root in C horizon. The surface horizon (A1) of GN soil with moderate, medium granular structure and many fine roots had matrix flow. The fingering occurred at the interfaces of sandy loam A horizon and loamy sand C horizon in GR soil and loam A1 horizon and sandy loam A2 horizon in GN soil. The LS soil with strong, coarse prismatic structure and the finest texture showed a macropore flow along cracks and had the deepest penetration of the dye tracer. The macropore (crack and vein), layer interface and plant root induced the preferential flow in the studied soils.

Keywords Crack · Fingering · Layer interface · Macropore flow · Matrix flow · Plant root · Vein

Received: 22 March 2004 / Accepted: 25 May 2004
Published online: 10 July 2004

J. G. Kim (✉) · C.-M. Chon · J.-S. Lee
Korea Institute of Geoscience and Mineral Resources,
30 Gajeong-dong Youseong-gu, Daejeon 305–350,
Korea
E-mail: jgkim@kigam.re.kr
Tel.: +81-42-8683658
Fax: +81-42-8619723

Introduction

Soil can act as a filter and can trap contaminants in the soil matrix preventing or reducing the contamination of groundwater. However preferential flow of water and solute in soil can allow contaminants to bypass the soil matrix and to proceed rapidly to groundwater (Flury and others 1994; Tindal and Vencill 1995). Preferential flow has been recognized as an important process for the transportation of water and contaminant in agricultural practice and environmental science (Flury 1996; Ogawa and others 1999). Flury and others (1994) examined the infiltration pattern of 14 field soils using an irrigation of dye tracer and excavation method. They found that structured soils were more prone to produce preferential flow and deeper penetration of tracer than unstructured soils. Three types of preferential flow (macropore flow, fingering and funnel flow) were recognized in unsaturated field soils (Beven and Germann 1982; Helling and Gish 1991).

The intensity of irrigation and rainfall and the moisture content of surface soil affect the formation of the preferential flow (German and DiPietro 1996; Gjettermann and others 1997; Quisenberry and others 1994). At low irrigation intensity and moisture content of surface soil, water in surface soil flows mainly due to the matrix potential that is limiting the preferential flow in subsoil. However, a positive pressure potential develops more extensively in surface soil initiating the preferential flow in subsoil under high irrigation intensity (Elliott and Coleman 1988). Macropore flow involves the transport of water through noncapillary large pores formed by dry and wet process, freeze and thaw cycles, soil fauna and plant root (Beven and Germann 1982). The size of macropores varies in a wide range between 30 and 3,000 μm (Stein and others 2001). Buttle and Leigh (1997) showed that larger macropores serve as more efficient conducts for preferential flow of water than smaller macropores. The soil with the higher density of macropore had the greater drainage area (Weiler and Naef 2003). Allaire-Leung and others (2000a, 2000b) demonstrated the effect of continuity and tortuosity of macropore on the infiltration pattern. Continuous macropore exhibited faster water conduction and conducted greater amounts of water than isolated macropore. They also showed that the macropore with the greater tortuosity had the greater retardation time and the greater infiltration of water to the surrounding matrix. Beven and

 DOI 10.1007/s00254-004-1108-y

Germann (1982) suggested that the rainfall intensity of 1–10 mm per hour might be sufficient to initiate macropore flow depending on the initial moisture content of surface soil. The macropore flow was triggered by intense rainfall (>5 mm per hour) even in a deep sandy loam with poorly developed structure (Simmonds and Northcliff 1998).

Hill and Parlange (1972) demonstrated first that fingering could occur in a fine over coarse textured soil. When the conductivity of the coarse-textured sublayer is greater than the rate of transmission through the fine-textured upper layer the flow velocity increases across the interlayer plane. The increased velocity leads fingering (Baker and Hillel 1990). Fingering was also reported in water repellent soils (Dekker and Ritsema 1994). The water repellency of a soil depends on the content of organic matter and water (Bisdom and others 1993; Dekker and Ritsema 1994). Fingering also occurs when the air pressure increases ahead of the infiltration front (Hill and Parlange 1972).

Funnel flow along the sloping interface of horizons was also recognized as an important phenomenon of preferential flows in subsurface soils (Walter and others 2000). Saturated interflow occurred in the upper layer underlain by a hydraulically restrictive layer such as massive bedrock (Stagnitti and others 1986). A capillary barrier developed at the sloping interface between the upper fine-textured layer and the lower coarse-textured layer also leads to a funnel flow (Kung 1990).

The flow of water in soils is not always uniform due to their three-dimensional heterogeneity (Mooney and others 1999; Smettem and Trudgill 1983; Weiler and Naef 2003). The infiltration of water and solute in soils by preferential flow could not be adequately described and predicted by models based on Darcian assumption (Beven and Germann 1982). Characterization of three-dimensional water and solute transport in a natural soil profile is not easy due to its textural and structural heterogeneous properties. Ghodrati and Jury (1990) demonstrated that the quantification of even the simplest parameter of solute transport in a soil profile such as mean and maximum depth of penetration was difficult using a coring method, the most common conventional characterization method. Numerous laboratory and field studies have been conducted to figure out the flow rate and pathway of water and solute in soil profiles.

Conservative inorganic ions such as bromide, chloride and nitrate have been used to trace water flow and contaminant migration in soils and aquifers. Dye tracing has also been employed to visualize flow paths and to mimic the transport behavior of adsorbing and nonadsorbing solutes (Flury and Jury 1995). The most commonly used dye tracer to stain flow paths in porous media is the nonfluorescent food dye Brilliant Blue FCF ($C_{37}H_{34}N_2Na_2O_9S_3$). Brilliant Blue FCF has a good visibility in soils and a weak adsorption on soils (Flury and Jury 1995). It also exhibits low toxicity and moderate price, making it a good tracer. The objective of this study was to examine the effect of textural and structural differences on the water infiltration pattern using Brilliant Blue FCF tracer at three field soils.

Material and methods

Characteristics of soil

Three uncultivated forest soils in Korea with different textures and structures were used for the field dye trace experiment. They were developed over a Jurassic granite (GR), a Precambrian gneiss (GN) and a Cambro-Ordovician limestone (LS) (Fig. 1). Structure of the soils was examined in the field. The soil color was recorded using a soil color reader (Minolta SPAD-503, Minolta Co. Ltd.). Three to four samples were collected from each soil profile based on horizon for the laboratory analysis of texture, mineralogy and chemical characteristics. The texture of the sample was determined using a laser particle analyzer (Mastersizer 2000, Malvern Co.) after removal of organic matter, carbonate and iron oxide (Jackson 1956). The mineralogical composition was determined using an X-ray diffractormeter (MAC Science MXP 18A Rint-2500). The acidity and electrical conductivity were determined using a 1 soil : 10 water method (Jackson 1956). The ignition loss as an indicator of organic matter content was determined by heating at 500°C for overnight.

Dye tracer test

A solution of Brilliant Blue FCF (Neveon Hilton Davis Inc., Cincinati, OH) at the concentration of 5 g l^{-1} was used to stain the flow paths (Reichenberger and others 2002). Before the application of the dye solution, the organic horizon was removed and the surface was leveled to reduce the effect of surface condition. Acryl square frame (1.0 × 1.0 m) was installed into the ground at a 5 cm depth (Fig. 2). The framed area was flooded with 150 L of the dye solution and was covered with a vinyl film to prevent

Fig. 1
Location map of the study sites: GN soil *(1)*, GR soil *(2)* and LS soil *(3)*

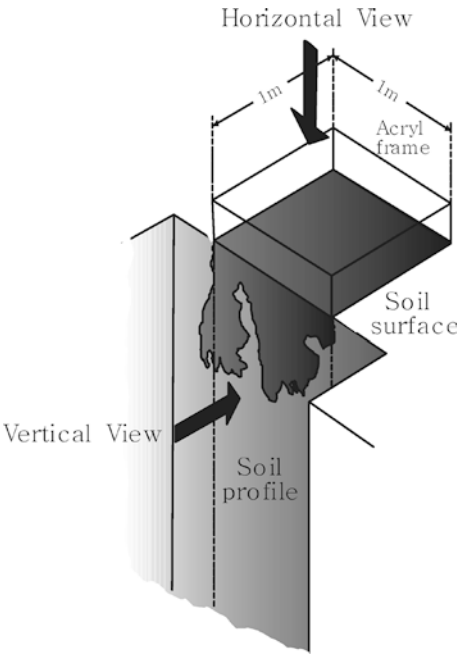

Fig. 2
Schematic presentation of the field dye tracer test

evaporation and dilution by rainfall. After 3 days of flooding, the soil was excavated down to a 1.5 m depth at an edge of the frame for the vertical view of the profile (Fig. 2). The horizontal views of the soil profile were exposed by removal of a 5 cm thick layer from the surface to 70 cm depth. The vertical and horizontal images were recoded using a digital camera (Sony Cybershot DSC-F717) under daylight. The same camera position was maintained for the horizontal image collection using an iron frame to minimize distortion differences between successive faces. The horizontal image of 80 × 80 cm for each layer, 10 cm away from the frame, was used for the image analysis to reduce the effect of boundary flow.

Image analysis

All image processing was conducted using a geographic image processing software, ER Mapper, Version 6.2 (Earth Resource Mapping Corporate, Australia). The pixel dimension of the photographs was resized with 1,200 by 1,200 pixels (80 × 80 cm) to normalize the resolution of each photograph. Because any arbitrary color can be represented as a composition of the three spectral densities in the red (R), green (G), and blue (B) range, only the Red-band of these colors selected and saved in a separate image plane with 256 gray values. After using the median filtering command of the program, the processed image was converted to black and white image plane, and finally the dye-stained pixel was classified. The dye coverage was determined by counting the stained pixels in the photograph (80 × 80 cm) for the horizontal view. For the dye coverage of the vertical view, the photograph was divided into slices (80 × 5 cm) with 5 cm depth increments and the stained pixels of each slice were counted.

Results and discussion

Characteristics of the soils

The characteristics of the soils are shown in Table 1. The three soils were acidic and had similar EC values. The color of three soils was yellowish red. The GR and GN soils had similar mineralogy (quartz, feldspar, mica, kaolinite and vermiculite) and the LS soil had quartz and kaolinite as major minerals. The values of ignition loss for the three soils ranged from 0.21 to 1.58%: the highest value for GN soil and the lowest value for GR soil. The GR soil had A and C horizons and the GN and LS soils had a deep A horizon. The LS soil had the finest texture (silty clay loam) and the GR soil had the coarsest texture (loamy sand). The A horizon of GR soil had a weak, medium granular structure and the C horizon had residual veins pegmatitic veins consisting of sand size mica and quartz that originated from the parent rock. The surface soil of the GN soil had moderate, medium granular structure and the subsurface soil had weak, medium subangular blocky structure. The LS soil had strong, coarse prismatic structure and the interpedal cracks had a high vertical continuity and a low tortuosity. The GR soil contained a few fine to coarse roots. The surface soil of GN contained many fine roots and the subsurface contained a few fine roots. The surface soil of LS contained a few fine roots and no root was observed in the subsurface soil. Any distinctive faunal burrows were not observed in the three soils.

The characteristic, texture and mineralogy of parent rocks were reflected in the characteristics of the soils. The texture and structure showed an apparent close relationship, i.e. the GR soil with coarse texture had a weak structure but the LS soil with fine texture had a good structure. The granite, the parent rock of GR soil, consisted of coarse-grained minerals such as quartz, muscovite and feldspar and had complex pegmatitic veins. The coarse texture and the residual rock structure in C horizon of GR soil are the apparent reflection of the characteristics of the parent rock. The weathering of the gneiss composed of fine-grained mica, quartz and feldspar might lead to the development of relatively fine-textured GN soil. The limestone mainly consisted of calcite and also contained trace amounts of fine-grained quartz and clay minerals. During the pedogenic process, calcite is dissolved out first and fine-grained quartz and clay minerals are enriched in soil due to the higher solubility of calcite than those of quartz and clay minerals. Therefore, the LS had fine texture resulting in a good soil structure (Buol and others 1980).

Stain image of vertical sections

Figure 3 shows the stain images of vertical cross sections for the three soils. For GR soil, the dye tracer penetrated down to a 65 cm depth (Fig. 3A) and horizontally infiltrated into 30 cm beyond the plot area along the interface of A and C horizons not presented in this paper. A homogeneous matrix flow occurred in the A horizon and a wavy front (fingering) of the matrix flow extended into C horizon. The macropore flow was also observed along the vein and plant root in C horizon. A dispersed pale staining

Table 1
Physical, mineralogical and chemical properties of the soils used in this study

Site	Classification[1]	P. material	Horizon	Depth (cm)	Color	Texture (clay/silt/sand) (%)	Structure	Mineralogy[2]	pH[3]	EC[4] (μS/cm)	LL[5] (%)
GR	Typic Dystrudepts	Granite	A	2–30	10YR 4/2	Sandy loam (3.3/30.0/66.7)	Weak, medium granular	Q, F, M, K	4.52	32.9	0.54
			C1	30–54	10YR 6/4	Loamy sand (2.6/20.4/77.0)	Residual rock structure	Q, F, M, K, V	6.07	25.0	0.46
			C2	54–150	10YR 6/4	Loamy sand (2.6/22.4/75.0)	Residual rock structure	Q, F, M, K, V	4.96	9.51	0.21
GN	Typic Dystrudepts	Gneiss	A1	3–12	5YR 3/4	Loam (10.3/49.7/40.0)	Moderate, medium granular	Q, K, M, F, V	4.74	27.5	1.58
			A2	12–74	2.5YR 3/4	Sandy loam (7.1/35.8/57.1)	Moderate, medium granular	Q, K, M, F, V	4.93	31.0	1.06
			A3	74–121	5YR 3/6	Silt loam (11.4/53.5/35.1)	Weak, medium subangular blocky	Q, K, M, F, V	6.41	20.2	1.10
			C	121–150	5YR 4/4	Silt loam (12.6/53.9/33.5)	Residual rock structure	Q, K, M, F, V	6.58	11.87	0.84
LS	Typic Hapludalfs	Lime-stone	A1	2–10	2.5YR 3/2	Silty clay loam(27.5/70.7/1.9)	Strong, coarse prismatic	Q, K, H	6.18	29.9	1.16
			A2	10–20	2.5YR 4/2	Silt loam (25.2/64.4/10.4)	Strong, coarse prismatic	Q, K, H	5.59	7.27	0.84
			A3	20–150	2.5YR 4/3	Silt loam (23.9/75.1/1.0)	Strong, coarse prismatic	Q, K, H	5.9	6.18	0.85

[1] adopted from NIAST and RDA (2000). [2] Q: quartz, F: feldspar, M: mica, K: kaolinite, V: vermiculite, H: hematite. [3] and [4] determined with 1soil and 10distiled water method. [5] Ignition loss

was observed in the surrounding area of the stained vein (Fig. 4A). At the end of preferential flow along the plant root, the dye stain showed a swelled and rounded bottom (Fig. 4B).

The front of the matrix flow in the GR soil (Fig. 3A) was apparently a match with the boundary of A and C horizons. When the wetting front arrives at the interface of finer-textured A horizon and coarser-textured C horizon, the downward movement of the wetting front temporarily stops at the interface due to the higher suction of A horizon and a lateral movement of the front may occur until the downward movement restarts (Baker and Hillel 1990). When the conductivity of the C horizon was greater than the rate of transmission through the A horizon, the fingering might occur at the layer interface. The dispersed pale stain might be the result of infiltration of conducting dye through the vein into the finer-textured surrounding matrix. The plant root induced a preferential flow (Devitt and Smith 2002; Hangen and others 2002) and the coarse-textured layer at the end of the root acted as a breaker for the preferential flow resulting in the swelled and rounded bottom (Yasuda and others 2001). Allaire-Leung and others (2000a) showed a high concentration of solute right below macropores in a soil.

The GN soil showed that the surface soil of a 10 cm depth was almost completely stained by the dye and a fingering was observed below that depth (Fig. 3B). The dye stain extended down to a 35 cm depth in the vertical view. The stain front was highly irregular and some isolated spots around plant roots were stained by the dye. The LS soil showed the most dramatic preferential flow pattern (Fig. 3C). Only the surface soil of a 2 cm depth was almost completely stained for the LS soil. Below that depth, macropore flow occurred along cracks and the dye penetrated to greater than a 150 cm depth (the maximum depth of vertical excavation for the site). The vertical image of LS soil also showed staining of interpedal faces (Fig. 4C). The thickness of infiltration into the surrounding matrix of cracks was less than 2 cm and it decreased with depth.

The depth of fingering in the GN soil matched well with the interface of finer-textured A1 (loam) and coarser-textured A2 (sandy loam) horizons. The textural difference between the adjacent two layers might induce the fingering as discussed above (Baker and Hillel 1990). The stained spots around plant roots in the GN soil indicate that a preferential flow occurred along the plant roots. The macropore flow along the cracks led the deepest penetration of the dye tracer in the well-structured and fine-textured LS soil (Flury and others 1994). The thin layer of stained matrix along the conducting crack indicates that the solute and contaminant may bypass to groundwater without the significant attenuation by the soil matrix resulting in groundwater contamination. The decreased thickness of the infiltration into the matrix with depth was due to the increased hardness of peds as observed in the field.

The calculated dye coverage with depth for the vertical section of the three soils is shown in Fig. 5. The dye coverage matches well with the visual observation of the

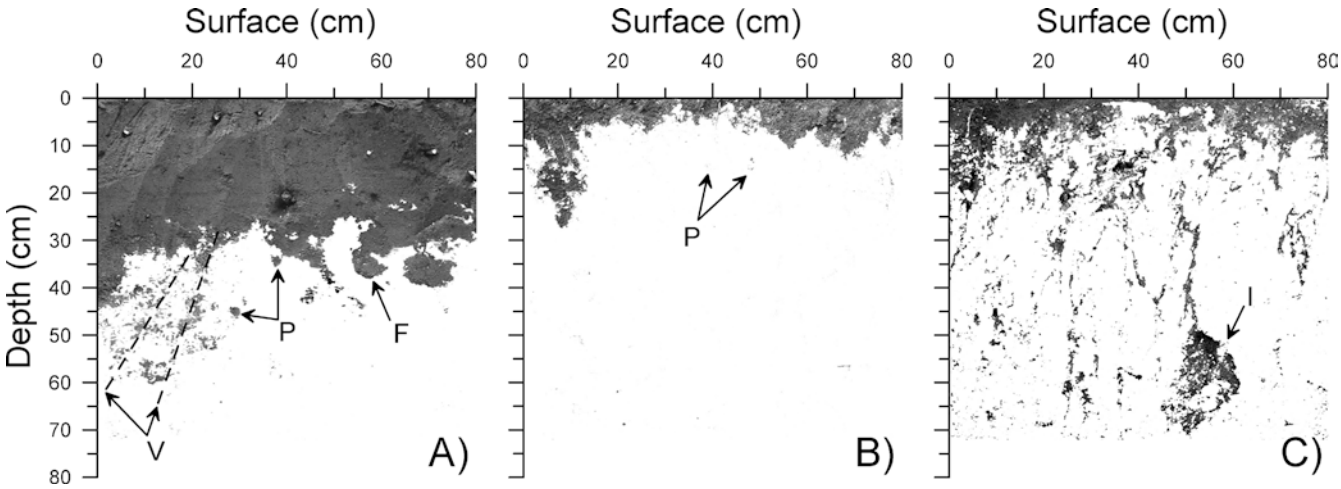

Fig. 3
The stained images of vertical sections of the three soils: GR soil **(A)** GN soil **(B)** and LS soil **(C)**. *P* represents for plant root in the figure; *F* for fingering; *V* for vein; *I* for interpedal face

vertical cross section. Matrix flow in surface soils showed the dye coverage of greater than 90%. A sharp decrease of dye coverage with depth showed just below the boundary of matrix flow and preferential flow. The dye coverage of the vertical face of LS soil sharply decreased with depth down to a 35 cm depth and then the dye coverage increased. The higher value of dye coverage showed at 55–70 cm depth of LS soil. The higher dye coverage was due to exhibition of the stained interpedal faces to the vertical cross section.

Stain image of horizontal section

For GR soil, the A horizon was almost completely stained by the dye and the dye stain extended down to a 65 cm depth (Fig. 6A). The stains along the vein and the plant root in C horizon were observed. The dye infiltration into the surrounding matrix of the vein and the coarse plant root was also observed. As observed in the stain image of the vertical cross section (Fig. 3 and 4), the vein and plant root act as a conducting route of the dye tracer resulting in a preferential flow (Devitt and Smith 2002; Weiler and Naef 2003). The pale stain around the vein observed in the vertical image (Fig. 3 and 4) might be related to the infiltration of the dye into the surrounding matrix. It was evident in horizontal images as well.

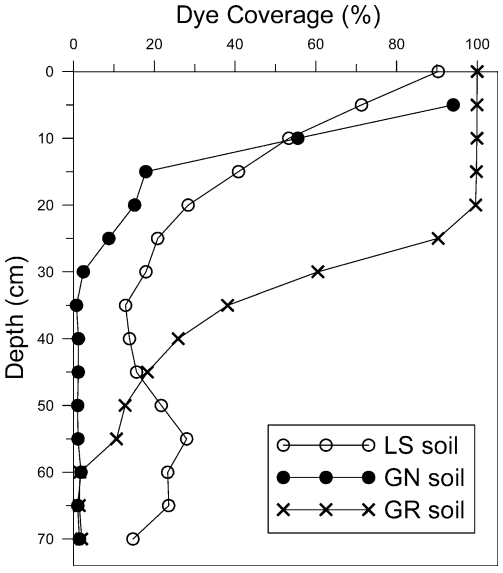

Fig. 5
Dye coverage of the vertical sections with depth

Almost all of the upper soil of a 10 cm depth of GN soil was stained and the dye tracer penetrated down to a 65 cm depth (Fig. 6B). The stained area of subsurface soil was dispersed on the horizontal faces. A linear-shaped stain along fine plant roots was observed in some areas. It indicates that the fine plant root acted as a conducting route of the dye tracer (Hangen and others 2002).

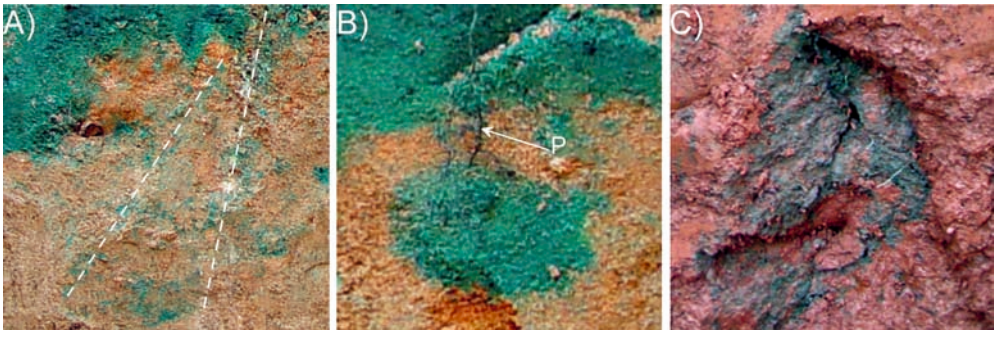

Fig. 4
The selected stained area of vertical section of GR and LS soils: pale staining around the vein of GR soil **(A)**, stain along and end of root of GR soil **(B)** and stained interpedal face of LS soil **(C)**. *Dashed lines* stand for the veins

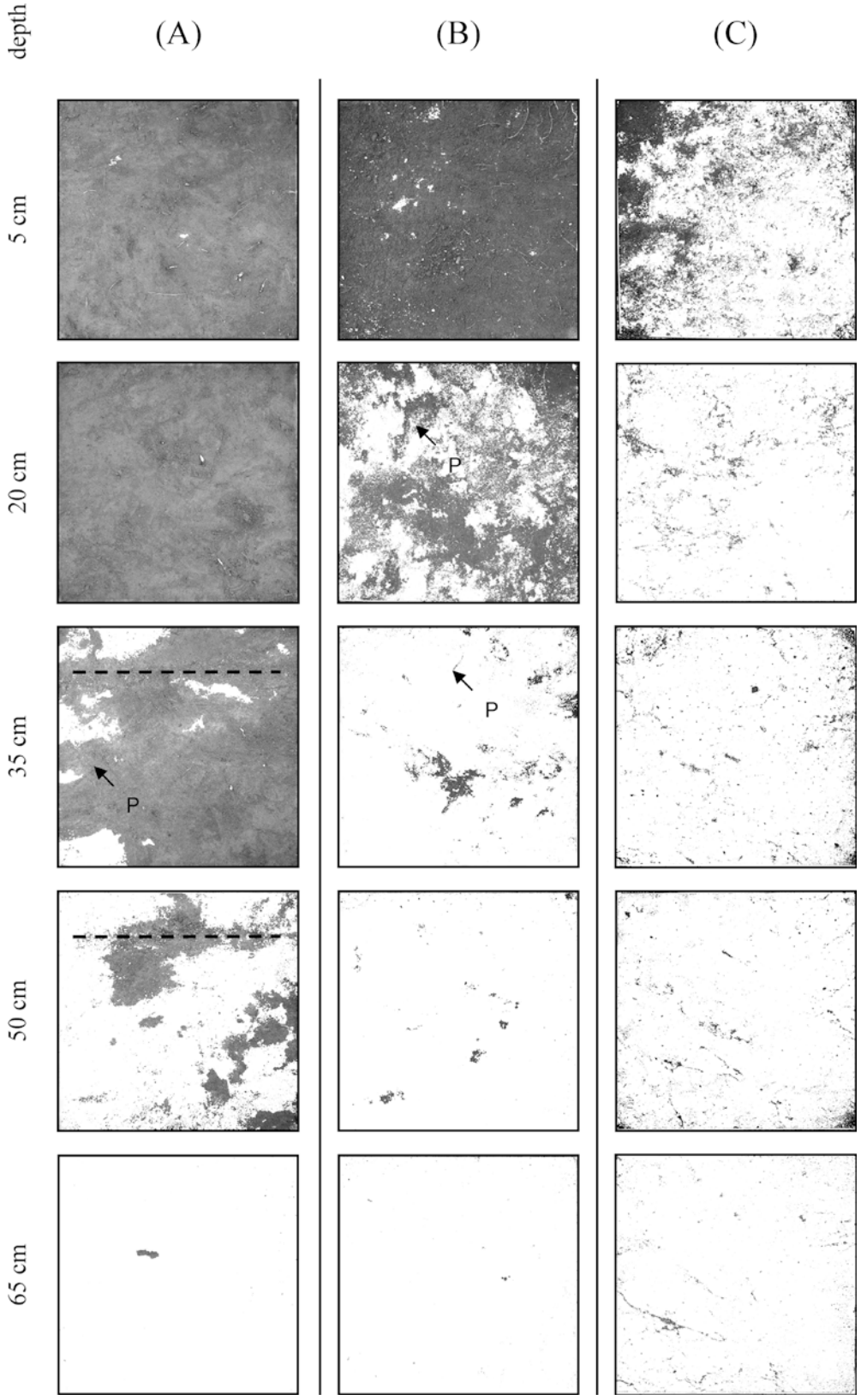

Fig. 6
Dye stained images of the horizontal sections: GR soil (**A**), GN soil (**B**) and LS soil (**C**). *V* stands for vein and *P* stands for plant root

Only the thin surface (<2 cm depth) of LS soil was almost completely stained and the LS soil showed the deepest penetration of the dye among the studied three soils (Fig. 6C). The horizontal stain image of LS soil showed both fuzzy and linear shapes and the linear shape became dominant with increasing depth. The width of the linear-shaped stain decreased with increasing depth. The prismatic peds in subsurface soil was harder than those in the

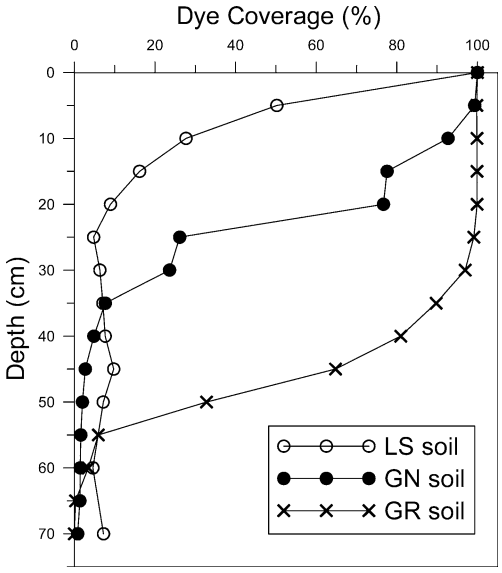

Fig. 7
Dye coverage of the horizontal sections with depth

surface soil observed in the field. It resulted in less extent of infiltration of dye into the surrounding matrix in subsurface soil. The horizontal stain image also indicates that matrix and macropore flows occurred only in the surface soil (0–10 cm depth) and a macropore flow along the cracks was the dominant flow pattern in subsurface soil. The dye coverage of the horizontal sections (Fig. 7) had a very similar pattern with the dye coverage of the vertical sections (Fig. 5) except the LS soil. The dye coverage of the horizontal section of LS soil showed a sharp decrease with increasing depth down to a 20 cm depth and then the dye coverage remained about 10% even though the depth increased down to 70 cm. The data of the horizontal dye coverage also strongly supports the flow pattern observed in the horizontal image.

Conclusions

The poorly structured surface soils of GR and GN showed a homogeneous matrix flow. A fingering was developed at the boundary of the finer-textured upper layer and coarser-textured sublayer of GR and GN soils. Plant roots in GR and GN soils induced a preferential flow. The coarse-grained pegmatitic vein originated from the parent rock in C horizon of GR soil also led a macropore flow with thick infiltration into its surrounding matrix. The LS soil with strong, coarse prismatic structure was dominated by the macropore flow along cracks. The LS soil showed the deepest penetration of dye tracer. A general conclusion is made for the water flow pattern for the three soils as followings:

1. The matrix flow occurred in the poorly structured surface soils;
2. the fingering occurred at the interface of the coarser layer over the finer layer;
3. veins originated from the parent rock and plant root led a preferential flow along them;
4. the well-structured soil showed the deepest penetration of the dye tracer among the studied soils.

Acknowledgements This study was supported by the Minister of Science and Technology, Korea (M1–0304–00–0001). The authors express a special thank to Mr. T.H. Kim for his help in the field and laboratory works.

References

Allaire-Leung SE, Gupta SC, Moncrief JF (2000a) Water and solute movement in soil as influenced by macropore characteristics: 1. Macropore continuity. Geoderma 41:283–301

Allaire-Leung SE, Gupta SC, Moncrief JF (2000b) Water and solute movement in soil as influenced by macropore characteristics: 2. Macropore tortuosity. Geoderma 41:303–315

Baker RS, Hillel D (1990) Laboratory tests of a theory of fingering during infiltration into layered soils. Soil Sci Soc Am J 54:20–30

Beven KJ, Germann PF (1982) Macropores and water flow in soils. Water Resour Res 18:1,311–1,325

Bisdom EBA, Dekker LW, Schoute JFT (1993) Water repellency of sieve fractions from sandy soils and relationships with organic material and soil structure. Geoderma 56:105–118

Buol SW, Hole, FD, McCracken, RJ (1980) Soil genesis and classification. The Iowa State University Press. Ames, IW

Buttle JM, Leigh DG (1997) The influence of artificial macropores on water and solute transport in laboratory soil columns. J of Hydrol 191:290–314

Dekker LW, Ritsema CJ (1994) How water moves in a water repellent sandy soil. 1. Potential and actual water repellency. Water Resour Res 30:2,507–2,517

Devitt DA, Smith SD (2002) Root channel macropores enhance downward movement of water in a Mojave Desert ecosystem. J of Arid Envrion 50:99–108

Elliott ET, Coleman DC (1988) Let the soil work for us. Ecological Bulletins. 39:23–32

Flury M (1996) Experimental evidence of transport of pesticides through field soils: A review. J Environ Qual 25:25–45

Flury M, Jury WA (1995) Tracer characteristics of Brilliant blue FCF. Soil Sci Soc Am J 59:22–27

Flury M, Fluhler H, Jury WA, Leuenberger J (1994) Susceptibility of soils to preferential flow of water: a field study. Water Resour Res 30:1,945–1,954

Germann PF, DiPietro L (1996) When is porous-media flow preferential? A hydromecanical perspective. Geoderma 74:1–21

Ghodrati M, Jury WA (1990) A field study using dyes to characterization preferential flow of water. Soil Sci Soc Am J 54:1,558–1,563

Gjettermann KL, Nielsen KL, Petersen CT, Jensen HE, Hansen S (1997) Preferential flow in sandy loam soils as affected by irrigation intensity. Soil Technology 11:139–152

Hangen E, Buczko U, Bens O, Brunotte J, Huttl RF (2002) Infiltration patterns into two soils under conventional and conservation tillage: influence of the spatial distribution of plant root structures and soil animal activity. Soil and Tillage Res 63:181–186

Helling CS, Gish TJ (1991) Physical and chemical processes affecting preferential flow. In: Gish TJ, Shirmohammadi A (eds) Preferential flow. Proc Natl Symp Chicago, IL. Dec. 16–17, 1991. Am Soc Agr ic Eng, St. Joseph, MI., pp 77–86

Hill DE, Parlange JY (1972) Wetting front instability in layered soils. Soil Sci Soc Am Proc 36:143–147

Jackson ML (1956) Soil chemical analysis-advanced course. Pub. by the author, Dept. of Soils, Univ. of Wis. Madision, WS, USA
Kung KJS (1990) Preferential flow in a sandy vadose zone. 2. Mechanisms and implications. Geoderma 46:59–71
Mooney SJ, Holden NM, Ward SM, Collins JF (1999) Morphological observations of dye tracer infiltration and by-pass flow in milled peat. Plant and Soil 208:106–178
Ogawa S, Baveye P, Boast CW, Parlange JY, Steenhuis T (1999) Surface fractal characteristics of preferential flow patterns in field soils: evaluation and effect of image processing. Geoderma 88:109–136
Quisenberry VL, Phillips RE, Zeleznik JM (1994) Spatial distribution of water and chloride flow in a well-structured soil. Soil Sci Soc Am J 58:1,294–1,300
Reichenberger S, Amelung W, Laabs V, Pinto A, Totsche KU, Zech W (2002) Pesticide displacement along preferential flow pathways in a Brazilian Oxisol. Geoderma 110:62–86
Simmonds LP, Northcliff (1998) Small scale variability in the flow of water and solutes and implications for lysimeter studies of solute leaching. Nutrient Cycling in Agroecosystems 50:65–75
Smettem KRJ, Trudgill ST (1983) An evaluation of some fluorescent and non-fluorescent dyes in the identification of water transmission routes in soils. J Soil Sci 34:45–56
Stagnitti F, Parlange MB, Steenhuis TS, Parlange JY (1986) Drainage from a uniform soil layer on a hillslope. Water Resour Res 22:631–634
Stein A, Van Leishout MNM, Booltink HWG (2001) Spatial interaction of methylene blue stained soil pores. Geoderma 102:101–121
Tindall JA, Vencill WK (1995) Transport of atrazine, 2,4-D, and dicamba through preferential flowpaths in an unsaturated claypan soil near Centralia, MO. J of Hydrol 166:37–59
Walter MT, Kim JS, Steenhuis TS, Parlange JY, Heilig A, Braddock RD, Selker JS, Boll J (2000) Funneled flow mechanism in a sloping layered soil: Laboratory investigation. Water Res 36:841–849
Weiler M, Naef F (2003) An experimental tracer study of the role of macropores in infiltration in grassland soils. Hydrol Process 17:477–493
Yasuda H, Berndtsson R, Persson H, Bahri A, Takuma K (2001) Characterizing preferential transport during flood irrigation of a heavy clay soil using the dye Vitasyn Blau Geoderma 100:49–66